Polymer Vol. 37 No. 7, pp. 1087–1093, 1996

0032-3861/96/$15.00+0.00

Imaging of polymer monolayers attached to silica surfaces by element specific transmission electron microscopy

A. Ribbe*, O. Prucker and J. Rühe†
Macromolecular Chemistry II, University of Bayreuth, 95440 Bayreuth, Germany and
**Bayreuth Institute for Macromolecular Research (BIMF), 95440 Bayreuth, Germany*

Transmission electron microscopy was used to study monolayers of polystyrene covalently attached to the surfaces of highly dispersed silica gels. The layers were grafted by using immobilized azo initiators and performing the polymerization reaction directly at the surface of the particles. Mono-energetic inelastically scattered electrons were used to map the silicon, oxygen and carbon distribution of the modified silica and create element specific images of the specimen. The micrographs give a direct image of the attached monolayers of the polymer molecules. From an analysis of the gray value profiles of the micrographs it can be concluded that the silica particles are surrounded by a continuous, polystyrene layer, approximately 10 nm thick.

(Keywords: polymer monolayers; silica surfaces; polystyrene; TEM)

INTRODUCTION

Polymer layers adsorbed on the surface of highly disperse materials such as silica have been studied by a large variety of different techniques. Infra-red (i.r.) spectroscopy under diffuse reflectance conditions (DRIFT)[1], solid-state nuclear magnetic resonance spectroscopy[2,3], X-ray photoelectron spectroscopy (X.p.s.)[4], and small-angle neutron scattering[5] are just a few examples of the methods[6] which have been used to elucidate the composition and thickness of the attached monolayers. Most of these methods, however, have very limited spatial resolution and the desired information can only be obtained about a large surface area. Direct observation of the attached polymer layer with both high vertical and lateral resolution (i.e. on a submicron level) cannot be achieved.

High-resolution images of modified particles can generally be obtained by transmission electron microscopy (TEM). However, a major obstacle for imaging of ultrathin polymer films is that frequently only a low contrast between particle, attached film and support can be observed and micrographs with sufficient resolution for imaging of monolayers are difficult to obtain when only light elements ($Z < 20$) are present. An enhancement of the contrast is possible, when element specific images[7–15] are generated. The element spectroscopic imaging (ESI) technique has been used for elemental mapping of a large number of biological[7,8] and to some extend polymeric, especially multiphase polymer, systems[9–13]. While conventional TEM uses elastically scattered electrons for generation of the micrograph image, ESI utilizes the inelastically scattered ones[14,15]. Electrons passing through the specimen undergo a specific energy loss ΔE depending on the elements present at the location of transit. The electrons are separated with respect to their energies and images are generated using these 'mono-energetic' electrons, thus showing the net element distribution in the samples.

In this paper ultrathin polystyrene layers covalently attached to highly disperse silica are studied by transmission electron microscopy with electron energy-loss (e.e.l.) spectroscopy and electron spectroscopic imaging (ESI). The aim of these studies is to investigate the composition, homogeneity and thickness of these films. The polymer monolayers are generated by immobilization of a radical chain initiator on the surface of the silica and subsequent polymerization ('grafting from'), which yields a monolayer of polymer covalently attached to the solid substrate.

EXPERIMENTAL

The silica employed in these studies (Aerosil A300, Degussa) had a specific surface area of $285 \pm 5\,m^2\,g^{-1}$ according to the Brunauer–Emmett–Teller (BET) nitrogen adsorption method and an average diameter of the primary particles of 7 nm. The primary particles form large aggregates of 0.1 to several μm diameter. An azo compound (4,4′-azobis(cyanopentanoic acid)) was immobilized on to the silica surface by using α,ω-functional silanes in a three-step synthesis. The structure of the polymer layer obtained in this way is schematically depicted in *Figure 1*. Using this method polystyrene films with graft densities of up to 10 g of polymer per g of silica could be attached. The covalently bound monolayers

† To whom correspondence should be addressed

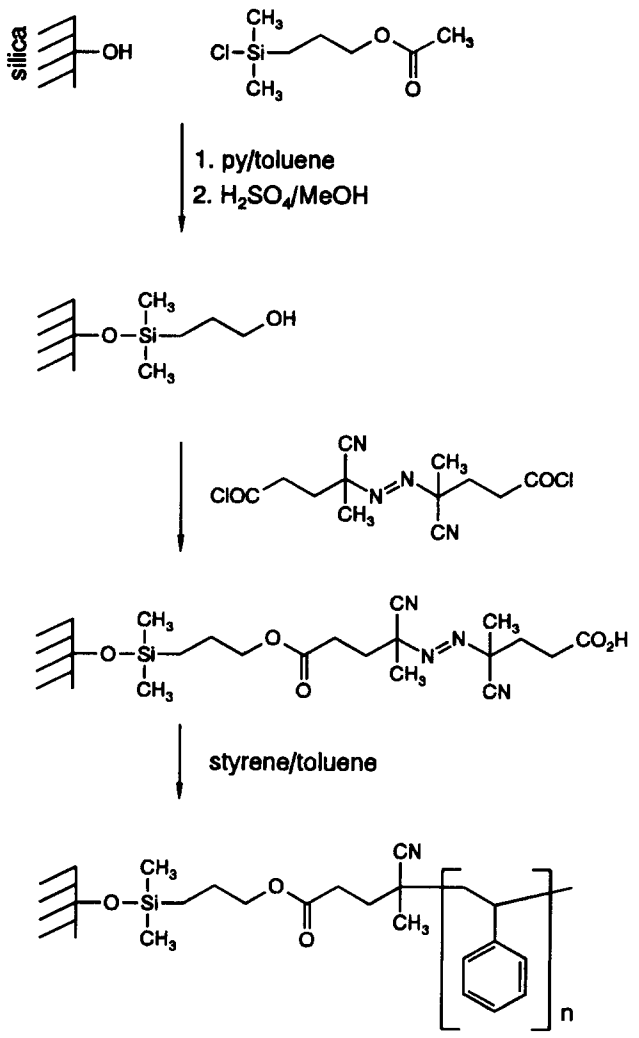

Figure 1 Preparation of the immobilized azo compound and polymer monolayer covalently bound to a silica surface

were characterized by using a variety of techniques, including diffuse reflectance i.r. spectroscopy, X.p.s., and elemental analysis. Details of the grafting reactions and characterization of the attached monolayers are described elsewhere[16,17].

The graft density of the sample chosen for this study was approximately 1 g of polymer per g of silica according to elemental analysis and was the lowest graft density of the materials synthsized. A material with a very low graft density was chosen on purpose, because with an increasing graft density the relative volume content of the silica substrate particles decreases strongly. Additionally, when relatively low graft densities were employed measurements of the film thickness by electron microscopy could be compared to the results of other methods of thickness determination, e.g. by X.p.s.

In order to measure the molecular weight of the attached polymer, the ester group connecting the polymer to the surface was cleaved off and the molecular weight of the degrafted material was determined by size exclusion chromatography to give $M_n = 160\,000\,g\,mol^{-1}$ (polydispersity, $M_w/M_n = 2.8$; calibration with narrow-molecular-weight polystyrene standards).

For the preparation of the electron microscopy specimen the unmodified silica gel was dispersed in water (1%) and the silica gel plus grafted polystyrene dispersed in chloroform (1 wt%). The solutions were stirred for 12 h. One drop of the obtained dispersion was placed on a carbon (10 nm) coated electron microscope grid (400 mesh) and the solvent was allowed to evaporate at room temperature.

The transmission electron microscopy investigations were carried out at a temperature of 110 K on a Zeiss CEM 902 instrument equipped with a Castaing-Henry filter lens, using an acceleration voltage of 80 keV. For e.e.l. spectrometry a photomultiplier was employed, while for image acquisition a video system was used. E.e.l. spectra were recorded on an area of 1600 nm^2 using a dwell time of $0.6\,s\,eV^{-1}$ (magnification = 250 000). Electron spectroscopic images were collected by a silicon-intensified target (SIT) camera (Dage Inc.). The intensity of the scattered electrons was assigned a gray value between 0 (black) and 255 (white). Image storage and image processing was carried out by using the IBAS 2.0 image system from Kontron. Except for background correction no other image processing was carried out.

No decay or alteration of the specimen was observed during image acquisition. The maximum electron dose during recording of the images was $\sim 0.04\,C\,cm^{-2}$. Although the occurrence of radiation induced processes such as crosslinking of the polymer is likely to occur[18], the dose to which the polymers have been exposed remained well below the characteristic dose for removal of carbon from comparable organic compounds at this temperature[19–21]. Repeated imaging of the same location and measurement of the thickness of the polymer film on the same particle showed no significant changes.

RESULTS AND DISCUSSION

Conventional TEM images (magnification =250 000) of unmodified and modified silica gels are depicted in *Figure 2*. Image (a) shows the silica without any surface modification, and image (b) the same material with a covalently bound polystyrene film. While the unmodified silica gel gives a clear image with sharp boundaries between particle and supporting carbon film, the image of the specimen with the grafted polystyrene (SiO_2–PS) appears somewhat blurred, although both micrographs were obtained under the same conditions. The low contrast between the attached layer and the support is probably due to the fact that both phases consist mostly of carbon and consequently the electron density differences are too small to give sufficient differences in scattering behaviour. While it can be clearly seen that the primary particles in the SiO_2–PS specimen are, as a result of the additional polymer layer, more than twice the size of the primary particles of the unmodified silica, the increase in size brought about by the attachment of the polymer monolayer is, however, difficult to quantify exactly. To circumvent this problem TEM studies using the electron spectroscopic imaging technique were carried out.

Typical e.e.l. spectra of an unmodified silica gel and of one with an attached polystyrene monolayer are shown in *Figure 3*. The location of the specimen, from which the spectrum of the polymer-modified silica was obtained, is encircled in the bright field image shown in *Figure 4d*. Both loss spectra show loss signals due to the presence of silicon ($Si_{L2,3}$ at 110 eV) and oxygen (O_K at 532 eV). The

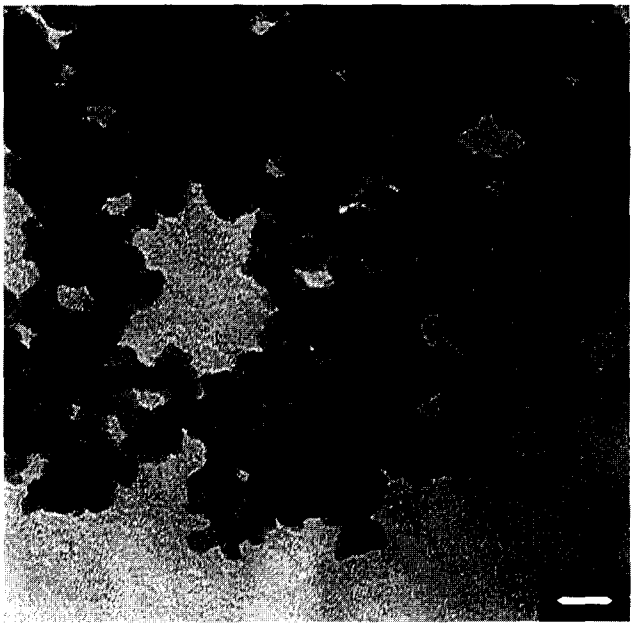

a

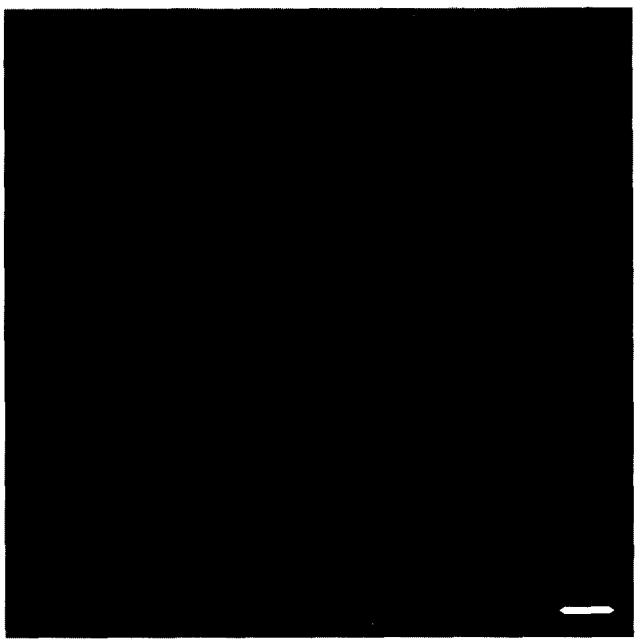

b

Figure 2 Transmission electron micrographs of (a) an unmodified silica gel and (b) silica with an attached polystyrene monolayer; magnification – 250 000, scale bar represents 20 nm

loss spectrum of the unmodified silica gel (upper trace) shows only a very weak carbon absorption signal (C_K at 284 eV) caused by the carbon support and/or carbon-containing impurities (carbon content of the unmodified silica <0.3 wt% according to combustion analysis) adsorbed on the particles. In contrast to this the silica plus grafted polystyrene (lower trace) shows a strong carbon signal due to the presence of the polymer monolayer.

This increase in the number of inelastically scattered electrons is used for image generation in the electron spectroscopic imaging technique[14,15]. As the image is constructed exclusively from inelastically scattered electrons, the intensity of the image is high in those regions where the element is present in the specimen in significant

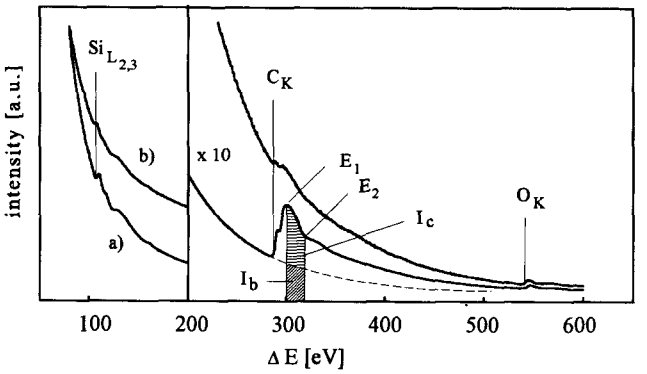

Figure 3 Electron energy-loss spectra of an unmodified silica particle (upper trace) and a silica gel plus a covalently bound monolayer of polystyrene (lower trace); dashed lines indicate extrapolated backgrounds; E_1 and E_2 are the upper and lower energy values, respectively, of the carbon image, while I_b is the background and I_c the carbon contribution to the overall intensity

concentrations. In all other regions the intensity is low and an element specific contrast is obtained.

However, the signal caused by the loss process cannot be used directly for image generation as it is superimposed on a descending background. Therefore, in order to obtain images with sufficient contrast, the background contribution I_b has to be subtracted from the total signal intensity.

The spectral intensity of an energy loss process can be described by the following:

$$I(E) = A\,e^{-r}\exp(-r) \qquad (1)$$

where A and r are parameters which depend on the energy and intensity of the inelastically scattered electrons and therefore on factors such as electron density and thickness of the sample[22,23]. Accordingly, they assume different values at every adsorption edge of the spectrum and also at different locations of the sample. The background contribution I_b to the total signal intensity of an ESI image can be calculated according to Egerton[22,23] as follows:

$$I_b = \frac{A}{(1-r)}(E_2^{1-r} - E_1^{1-r}) \qquad (2)$$

where E_1 and E_2 are the lower and the upper energy limit, respectively, of the energy window for generation of the element image.

The position of the absorption edges, and the energies at which element and reference images were recorded, are summarized in *Table 1*. Two reference images were taken at energies below the adsorption edge and the background contribution I_b to the intensity of the 'as-obtained' element image calculated according to equation (2) for each pixel. The extrapolated background signals obtained were digitally subtracted from the total intensity and the net intensity I_c for each pixel of the image was then obtained ('three-image method'). *Figure 4a* shows a typical image of the net carbon distribution of an agglomerate of SiO_2–PS after background subtraction. The image was recorded at a magnification of 140 000. The polymer layer attached to the silica can be seen as a white area around the image of the silica particles, where the latter appear black. The gray value of each pixel of the image represents an intensity $I(\Delta)$, which is specific

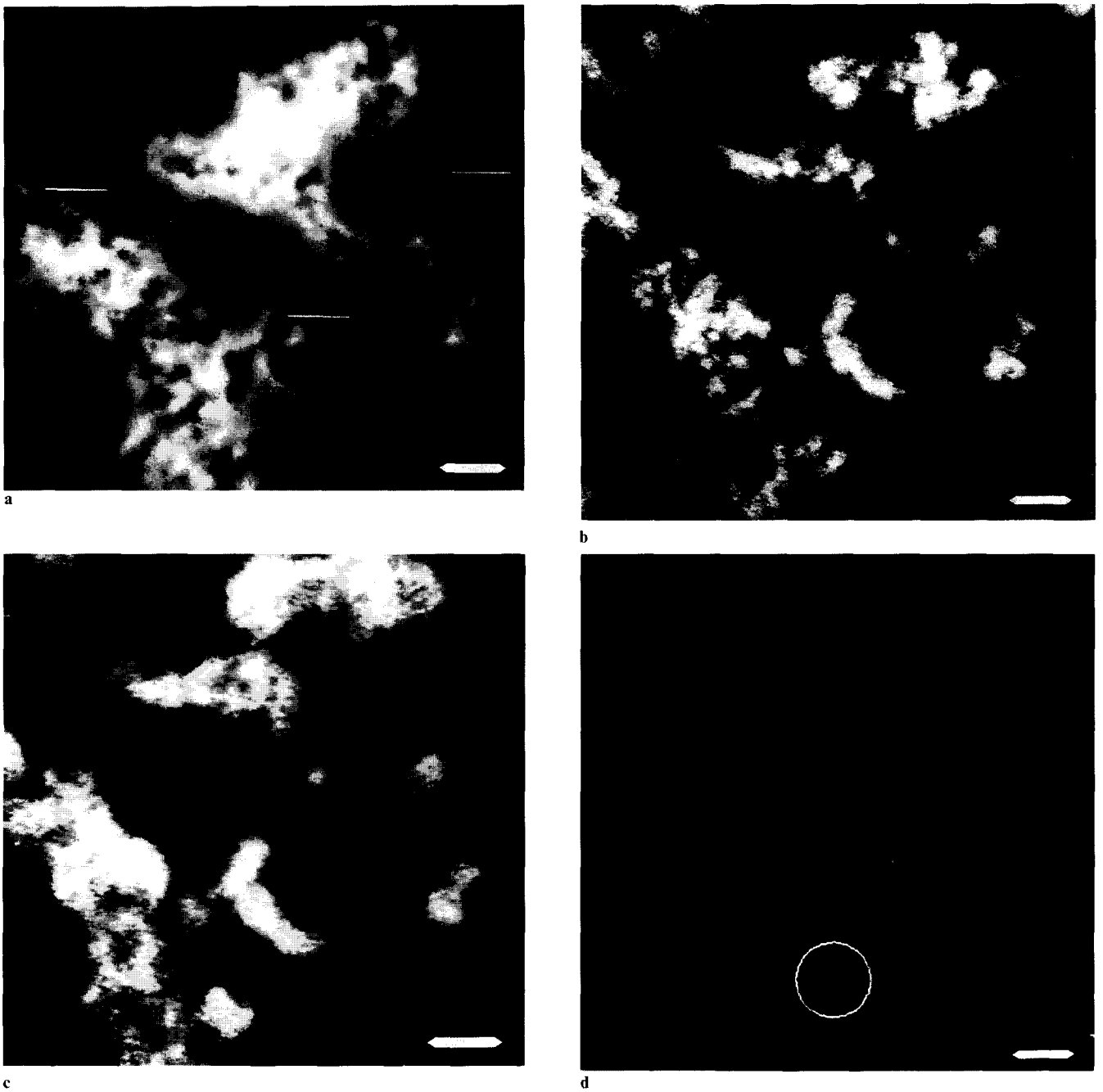

Figure 4 Electron spectroscopic images of a monolayer of polystyrene covalently bound to a silica surface, showing (a) carbon, (b) silicon and (c) oxygen distributions; bright areas indicate high, while dark areas indicate low concentrations of element contents, with the lines showing the regions from which gray value profiles were obtained. (d) Bright field image of the same area as (a)–(c) at a magnification of 140 000 (encircled area shows region where spectrum of *Figure 3* was taken); scale bar represents 40 nm (see text for further details)

Table 1 Values obtained for the absorption edge ΔE of elements present in the polymer-modified silica gels and energies of the element and reference micrographs used for element spectroscopic imaging of the samples

Element	ΔE (eV)	Energy (eV)		
		Reference 1	Reference 2	Element
Carbon	−284	−260	−270	−300
Oxygen	−532	−515	−525	−550
Silica	−99	−80	−90	−120

to the loss process and directly correlated to the element contents N of the measured location according to the following[23]:

$$I(\Delta) \cong N\sigma(\Delta)I_1(\Delta) \tag{3}$$

where $I_1(\Delta)$ is the intensity present in the region with low energy loss, σ is the reduced cross-section, and Δ is the energy range from E to $E + \Delta$.

When particles at the edge of the agglomerates are studied, it can be clearly seen that the polymer layer around the silica particles is continuous. While many different locations in a large number of silica aggregates were analysed no location could be detected where

coverage of the substrate with the polymer layer was incomplete.

In the centre of the silica agglomerates the interpretation of the micrographs is not straightforward, because in some of those areas the thickness of the specimen is so large that multiple scattering of the electrons occurs. In this case, the gray value of the image is not directly correlated to the carbon content of the specimen. Multiple scattering occurs when the sample thickness t of the specimen becomes comparable or larger than the mean free path of the electrons, and for large values of t/λ the intensity is no longer directly correlated to the element concentration as described in equation (3).

In this case, the intensity of the inelastically scattered electrons becomes very strongly dependent on the local thickness of the specimen. Eventually, it will even decrease with increasing thickness as the fraction of elastically scattered electrons increases, as follows[24]:

$$I_i = I \exp(-t/\lambda_e)[1 - \exp(-t/\lambda_i)] \quad (4)$$

where λ_i and λ_e are the mean free paths, respectively, of the elastically and inelastically scattered electrons. Therefore, a quantitative analysis was carried out only on particles at the edges of agglomerates, where the thickness of the specimen was sufficiently low.

Although the silica particles are completely surrounded by the attached polymer layer, electrons passing through the core of the particles are much more likely to be scattered than those passing only through the polymer shell as a result of the larger scattering cross-section of the silicon and oxygen atoms compared to the carbon and hydrogen of the polymer film. Therefore at those locations where silica is present, fewer electrons reach the detector and the image appears black, despite the fact that carbon is present both on top and below the particles.

This interpretation is directly confirmed when the images of the silicon (*Figure 4b*) or oxygen distribution (*Figure 4c*) and the bright field image (*Figure 4d*) of the same location are compared to that of the carbon distribution (*Figure 4a*). *Figures 4b* and *4c* were generated by using mono-energetic electrons inelastically scattered at silicon (*Figure 4b*) or oxygen atoms (*Figure 4c*). The same technique as described above for the net carbon distribution was applied. It is only at locations where silica is present that the intensities I_{Si} and I_O are high, and therefore only these locations appear white in the net element distribution.

In the bright field image (*Figure 4d*) the silica particles appear black. This is due to their higher atomic number and therefore larger scattering cross-section of the silicon and oxygen atoms in the particles when compared to the polymer, which consists of carbon and hydrogen atoms only. The increased scattering cross-section leads to an increase in the ratio of elastically vs. inelastically scattered electrons and a smaller number of electrons reaching the detector.

When primary particles at the edge of the agglomerate are analysed, the gray value profile of the carbon distribution gives direct information about the polymer layer thickness. Traces, along which the gray value profiles were recorded, are depicted as white lines in *Figure 4a*. As shown in *Figure 5*, the signals due to the carbon content of the specimen are superimposed on a descending background. This decrease of the signal intensity from the middle to the edges of the image is due

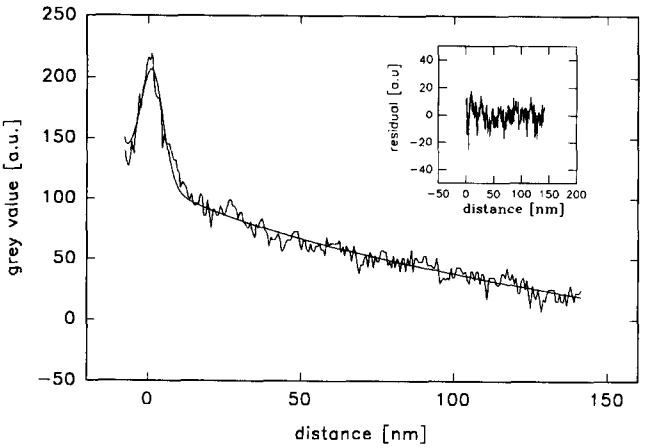

Figure 5 Gray value profile of the net carbon image along the trace indicated in *Figure 4*, where the straight line shows the curve fit; for the background contribution a square-root function was used, while for the signal exponential functions were employed. Insert depicts the difference between the measured data and the curve fit

to the intensity profile of the illuminating beam. The absolute number of electrons passing through the specimen is not the same in all locations, but varies with respect to the distance to the optical axis of the microscope. The strongest intensity of the electron beam is in the centre of the irradiated areas and decreases out to the edges.

From an analysis of the gray value profiles the thickness of the attached monolayer can be directly estimated. The highest gray value is obtained directly at the interface between the silica particle and the polymer layer, as schematically depicted in *Figure 6a*. When a trace is followed from the interface through the polymer layer, the gray value decreases with increasing distance from the surface of the silica particle. This decrease is caused by a convolution of the sample geometry and the segment density profile of the attached macromolecules. When the trace is followed in the opposite direction (i.e. to the centre of the silica particles) the intensity drops off rapidly, due to the fact that more and more electrons are scattered by the particles and fewer electrons reach the detector.

The thickness of the polymer layer can be obtained directly from the image, when the distance is measured where the value of the intensity of the gray value profile of the carbon signal reaches zero after background correction. This average distance was measured to 10 ± 2 nm in many different locations of the sample and was very well reproducible when different samples having the same graft density, and which were prepared by the same experimental procedures, were studied.

This thickness value for the polymer layer obtained from the element specific electron microscopic images was found to be in good agreement with the calculations of the layer thickness from X-ray photoelectron spectrometry (X.p.s.) measurements[16,17]. The attachment of the polymer layer causes a strong attenuation of the signals of the silica substrate. An analysis of the relative signal intensity of the Si1s and Si2p (substrate) signals, compared to that of the C1s signal of the attached polystyrene films gave good agreement with the electron-microscopy-analysis thickness values of 8 nm for the attached polymer film, depending on the preparation and

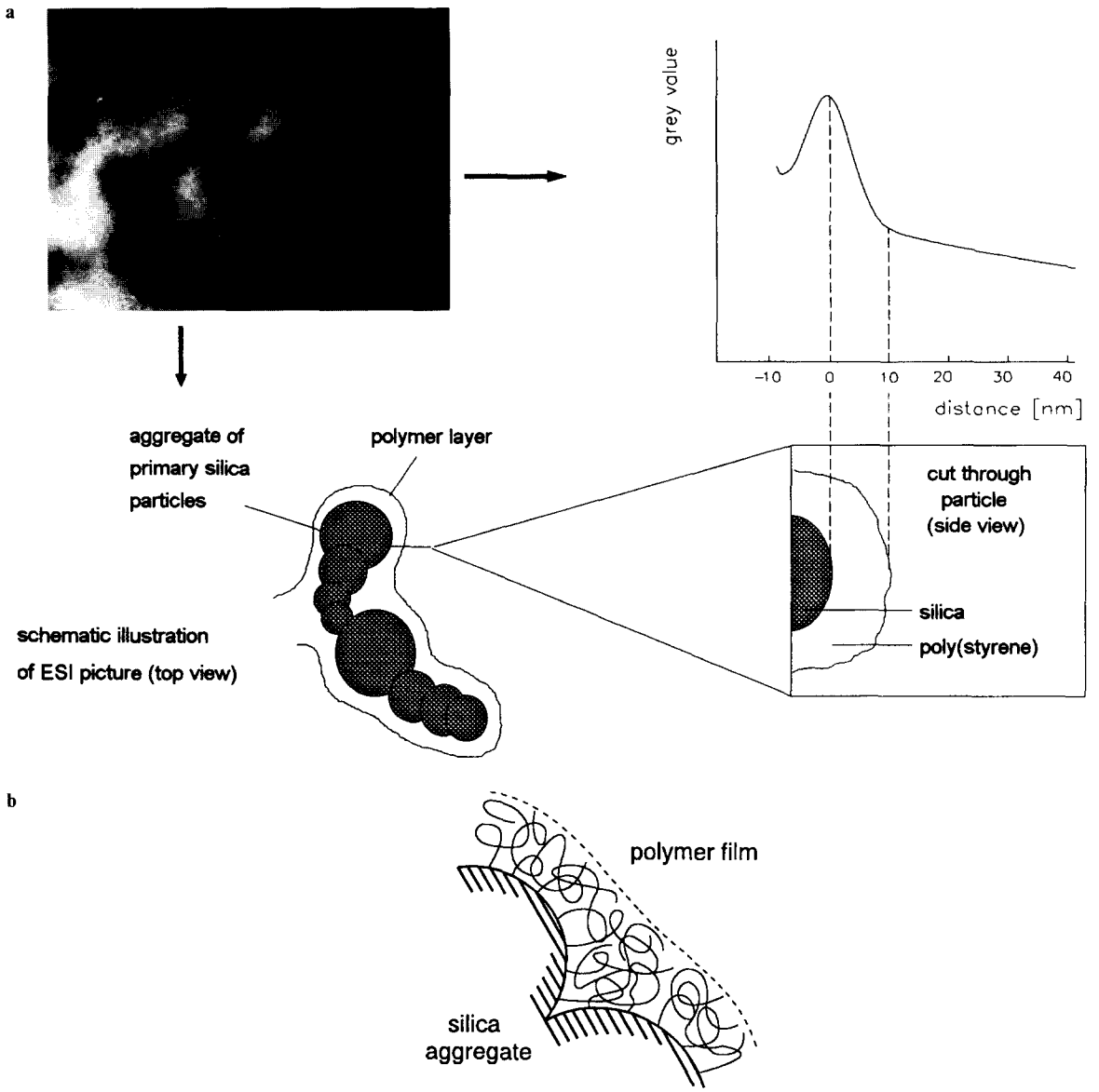

Figure 6 (a) Schematic description of gray value profiles of ESI micrographs. (b) Illustration of differences in the conformations of tethered polymer molecules grafted to locations with positive (spheres) and negative (pores) curvatures

polymerization conditions. In films with thicknesses larger than 10 nm substrate signals are no longer visible and no thickness determination by X.p.s. can be performed.

However, it should be noted that upon careful measurement of the film thickness by ESI it was observed that the polymer layer thickness in the pores, created by aggregation of the primary particles, was somewhat larger (depicted schematically in *Figure 6a*). This can be easily understood when it is considered that the polymer chains in the pores are much more crowded and therefore have to assume a geometry different to those on the positively curved surfaces. It has been theoretically predicted[25–27] that the terminal attachment of polymer molecules with a small distance between the graft sites leads to a stretching of the polymer coils perpendicular to the surface. This stretching is driven by the concentration gradient between the (solvent-filled) immobile polymer layer and the pure solvent surrounding the polymer-modified particles. As the polymer chains are covalently bound to the surface they cannot diffuse away, but solvent molecules diffuse into the polymer layer to decrease this gradient, leading to an extension of the polymer molecules perpendicular to the surface. This stretching is counterbalanced by the elastic forces of the chains, as the elongation of the chain is energetically unfavourable for entropic reasons (decrease of the number of possible conformations)[25–27]. On positively curved surfaces the concentration gradient, and consequently the driving force for the stretching of the molecules, becomes rapidly smaller with an increasing distance from the surface as more and more volume becomes accessible for the chains. Inside those pores having dimensions close to those of the tethered chains, however, the situation is completely different. With an increasing distance from the surface no further volume becomes accessible, but instead more chains compete for the same volume (*Figure 6b*). Therefore the conformation of the polymer chains on concave surfaces should be on average more stretched thus leading to a filling of the

pores and a strong decrease in the surface area of the aggregates.

This strong decrease in the surface area can be directly seen when the specific surface of the polymer modified particles is measured by the BET method. It is observed, that the specific surface area is reduced upon grafting of the polymer monolayer, from $160\,m^2\,g^{-1}$ for the SiO_2 with the immobilized azo compound to $<10\,m^2\,g^{-1}$ after attachment of the polymer.

It should be noted that the thickness value obtained by the electron microscopic measurements is that of a polystyrene film in high vacuum and therefore the polymer molecules are in a solvent-free, collapsed state. When films consisting of polymer molecules deposited by attachment of preformed polymer molecules with functional groups to appropriate reactive sites of the surfaces of substrates (the 'grafting-to' technique), or simply by physical adsorption, only layer thicknesses of 3 to 5 nm can be obtained[28]. The thickness value of 10 nm for films prepared by the method described in this paper is not the maximum which can be achieved by this method. As already mentioned above the graft density of the film studied here was on of the lowest prepared in a large series of experiments.

The direct measurement of the film thickness, where the molecular weight and graft density of the polymer chains on the surface can be measured on the same sample, allows a detailed insight into the behaviour of polymer chains tethered to a solid surface of highly dispersed materials. Studies on such tethered polymer chains, with a large variation in molecular weight and graft density of the attached polymer molecules, have been carried out and will be described in a subsequent communication[29].

CONCLUSIONS

Transmission electron microscopy with an element spectroscopic set-up, which allows the generation of element specific images, offers many new possibilities for the characterization of ultrathin films attached to the surfaces of highly dispersed particles. When inelastically scattered, mono-energetic electrons are used, images with high contrast between the attached layer, substrate and support can be obtained. The chemical composition of the attached film can be mapped and the homogeneity of the bound ultrathin layer can be measured with high spatial resolution. Even very local changes in the composition of an attached polymer layer should be easily detected when they are accompanied by corresponding changes in the element distribution. Analysis of the gray value profile allows the direct measurement of the thickness of the bound film.

The application of this technique to the study of ultrathin films attached to surfaces of solid materials holds great promise for the characterization of these layers at a submicron level.

ACKNOWLEDGEMENTS

J. Rühe is indebted to the 'Fonds der Chemischen Industrie' for a Liebig Fellowship. Financial support by the German Science Foundation (Deutsche Forschungsgemeinschaft) is gratefully acknowledged. The authors wish to thank the SFB 213, University of Bayreuth, for the kind use of the TEM facilities. Professor C. D. Eisenbach is also thanked for his interest in this work.

REFERENCES

1 Fontana, B. and Thomas, J. *J. Phys. Chem.* 1962 **65**, 480
2 Barnett, K. B., Cosgrove, T., Vincent, B., Sissons, D. S. and Cohen Stuart, M. *Macromolecules* 1981, **14**, 1018
3 Litvinov, M. and Spiess, H. W. *Makromol. Chem.* 1992, **193**, 1181
4 Lenk, T. J., Hallmark, V. M., Rabolt, J. F., Häussling, L. and Ringsdorf, H. *Macromolecules* 1993, **26**, 1230
5 Auroy, P. and Auvray, L. *J. Phys. II* 1993, **3**, 227
6 For a recent review see Fleer, G. J., Cohen-Stuart, M. A., Scheutjens, J. M. H. M., Cosgrove, T. and Vincent, B. 'Polymers at Interfaces', Chapman and Hall, London, 1993, p. 43
7 *Ultramicroscopy* 1990, **32**, special issue dedicated to 'Electron Spectroscopic Imaging and Analysis Technique'
8 *J. Microsc.* 1991, **162**, special issue dedicated to 'Electron Spectroscopic Imaging'
9 Cantow, H. J., Kunz, M. and Möller, M. *Makromol. Chem. Rapid Commun.* 1987, **8**, 401
10 Kunz, M., Möller, M., Heinrich, U.-R. and Cantow, H.-J., *Makromol. Chem., Makromol. Symp* 1989, **23**, 57
11 Cantow, H.-J., Kunz, M., Kunz, S. and Möller, M. *Makromol. Chem., Makromol. Symp.* 1989, **26**, 191
12 Eisenbach, C. D., Heinemann, T., Ribbe, A. and Stadler, E. *Angew. Makromol. Chem.* 1992, **202/203**, 221
13 Samseth, J., Mortensen, K., Burns, J. L. and Spontak, R. J. *J. Appl. Polym. Sci.* 1992, **44**, 1245
14 Egerton, R. F. 'Electron Energy Loss Spectroscopy', Plenum, New York, 1986
15 Obbensmeyer, F. P., Andrews, D. W., Arsenault, A. L., Heng, Y. M., Simon, G. T. and Weatherly, G. C. *Scanning* 1988, **10**, 227
16 Prucker, O. and Rühe, J. *Proc. Mater. Res. Soc.* 1993, **304**, 167
17 Prucker, O. and Rühe, J., unpublished results
18 Ditchfield, R. W., Grubb, D. T. and Whelan, M. J. *Philos. Mag.* 1973, **27**, 1267
19 Misra, M. and Egerton, R. F. *Ultramicroscopy* 1984, **15**, 337
20 Egerton, R. F. in 'Analytical Electron Microscopy' (Ed. R. H. Geiss), San Francisco Press, San Francisco, 1981, p. 154
21 Reimer, L. 'Transmission Electron Microscopy', 3rd Edn, Springer Series in Optical Science, Springer, Berlin, 1993, p. 439
22 Egerton, R. F. 'Electron Energy Loss Spectroscopy', Plenum, New York, 1986, p. 258
23 Egerton, R. F. 'Electron Energy Loss Spectroscopy', Plenum, New York, 1986, p. 265
24 Egerton, R. F. *Ultramicroscopy* 1982, **9**, 297
25 de Gennes, P. G. *J. Phys. (France)* 1976, **37**, 1443
26 Alexander, S. *J. Phys. (France)* 1977, **28**, 977
27 Halperin, A., Tirell, M. and Lodge, T. P. *Adv. Polym. Sci.* 1992, **100**, 31
28 Fleer, G. J., Cohen-Stuart, M. A., Scheutjens, J. M. H. M., Cosgrove, T. and Vincent, B. 'Polymers at Interfaces', Chapman and Hall, London, 1993, Ch. 8, p. 376
29 Ribbe, A. and Rühe, J., unpublished results